Main group metal halide complexes with sterically hindered thioureas
XIII. Crystallographic study of a unique cross-linked polymeric dichlorolead(II) complex with 1,1′-methylenebis(3-methyl-2(3*H*)-imidazolethione)

Daniel J. Williams*, Ali Shilatifard
Department of Chemistry, Kennesaw State College, Marietta, GA 30061 (USA)

Donald VanDerveer, Leigh Ann Lipscomb
School of Chemistry, Georgia Institute of Technology, Atlanta, GA 30332 (USA)

and Robert L. Jones
Department of Chemistry, Emory University, Atlanta, GA 30332 (USA)

(Received February 18, 1992; revised June 26, 1992)

Abstract

Two complexes, $PbCl_2$mbit and $Pb(NCS)_2$mbit (mbit = 1,1′-methylenebis(3-methyl-2)3*H*)-imidazolethione)) have been synthesized and characterized. A single crystal X-ray study of $PbCl_2$mbit revealed a unique cross-linked polymeric structure composed of very distorted $PbCl_4S_2$ octahedra sharing common edges through long Pb-Cl bridges. The bridging pairs of Cl atoms are displaced *cis* to each other in the coordination sphere of lead thus creating twisted polymeric Pb–Cl strands running along the *c* axis. In the direction of the *b* axis, the strands are further linked by mbit ligands acting as bridges between neighboring twisted strands created by the lead chloride bonds. This is the first instance where mbit is shown to act a bridging ligand. There is no clear evidence for the lone pair of electrons through systematic distortions in the lead coordination sphere. A high melting point of 259–261 °C is consistent with the polymeric structure. Cell parameters are as follows for $PbCl_2$mbit: space group *Pbca*, $a = 8.699(3)$, $b = 17.164(4)$, $c = 20.469(6)$ Å, $Z = 8$, $V = 3056.2$ Å^3, $D_c = 2.254$ g/cm$_3$, $D_o = 2.23$ g/cm^3 ($\lambda = 0.71073$ Å). $R = 0.047$. $Pb(NCS)_2$mbit complex was also synthesized and characterized, but crystals suitable for X-ray study were not obtained. IR stretching frequencies of the SCN group fall in the ranges observed for this ligand bonding only through N and no evidence for S bonding. The relatively high melting point (254–256 °C) gives evidence for a polymeric structure the details of which remain unknown.

Introduction

In part XI of this series, we reported the synthesis and characterization of a new bidentate ligand, 1,1′-methylenebis(3-methyl-2(3*H*)-imidazolethione) (mbit, see Fig. 1), as well as the synthesis and characterization of two new 1:1 complexes with Sb(III) and Bi(III) chloride including the results of a single crystal X-ray study for $SbCl_3$mbit. The X-ray study revealed a distorted octahedral coordination sphere about the antimony, and the mbit was functioning as a bidentate ligand to form an eight-membered ring with the central metal included [1]. Since that time, we have synthesized and characterized a few other new compounds with this novel sulfur-based ligand including two PbX_2 complexes where X = Cl and NCS. The purpose of this paper is report the synthesis and characterization of these new complexes and to give the results of a single crystal X-ray study for $PbCl_2$mbit.

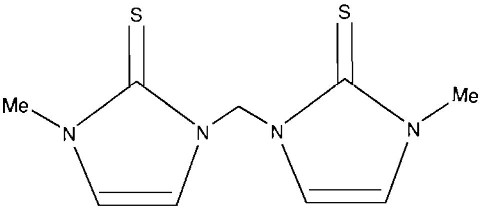

Fig. 1. 1,1′-Methylenebis(3-methyl-2(3*H*)-imidazolethione) (mbit).

---

*Author to whom correspondence should be addressed.

Experimental

Chemicals

All chemicals were reagent grade and used as commercially obtained without further purification. Spectroscopic grade CD_3CN (Aldrich) was used as a solvent to obtain the proton NMR data. mbit and $Pb(NCS)_2$ were synthesized as previously reported [1, 2].

Analytical

Carbon, hydrogen, nitrogen and halogen analyses were done by Atlantic Microlabs, Inc.

Solution studies

Proton NMR were recorded in CD_3CN on a 300 MHz GE model QE-300 FT-NMR spectrometer. Chemical shifts are reported in ppm (δ) relative to external tetramethylsilane. Key: s-singlet, d = doublet. Conductivity studies were not done.

Solid state spectra

IR spectra were recorded as mineral oil (Nujol) mulls between AgCl plates from 4000 to 400 cm^{-1} on a Mattson Galaxy 2020 Fourier transform infrared spectrophotometer (FT-IR). Raman data were collected from 3500 to 50 cm^{-1} on powders using a Bruker IFS-66 FT-Raman spectrophotometer equipped with Nd-YAG laser ($\lambda_{ex} = 1.063$ μm). All values are reported in cm^{-1} (± 4). Key: v = very, w = weak, m = medium, s = strong, br-broad, sh = shoulder. Only the observed peaks up to *c*. 2000 cm^{-1} are reported here for both the FT-IR and Raman spectra.

Synthesis

Melting points (uncorrected) were obtained on a Fisher-Johns stage-type apparatus and are reported in degrees Celsius.

[1,1'-Methylenebis(3-methyl-2(3H)-imidazolethione)]-dichlorolead(II)

Equimolar quantities of $PbCl_2$ and mbit (5.00 mmol each; 1.20 and 1.39 g, respectively) were dissolved separately in boiling water (75.0 and 50.0 ml, respectively). The two solutions were mixed with stirring and kept at boiling for *c*. 10 min. Following hot filtration, the mixture was reduced to half volume and allowed to cool. White crystalline needles were filtered and allowed to dry. The crystals were washed with a few small aliquots of CH_2Cl_2 on a sintered glass filter. Upon suction filtration and air-drying, 1.13 g of pure product remained (43% yield). Crystallographic grade crystals were grown by slow cooling hot aqueous solutions. m.p. 259–261 °C. *Anal.* Calc. for $C_9H_{12}Cl_2N_4PbS_2$: C, 20.85; H, 2.33; N, 10.81; Cl, 13.68. Found: C, 20.92; H, 2.37; N, 10.77; Cl, 13.62% ^1H NMR (δ): 3.47 (s, 3, methyl), 6.18 (s, 1, methylene), 6.79 (d, 1, $J_{AB} = 3$ Hz, ethylenic), 7.43 (d, 1, $J_{AB} = 3$ Hz, ethylenic). IR (Nujol mull): 1561w, 1313m, 1256w, 1226s, 1204m, 1159m, 1087w, 1067w, 1045w, 1020vw, 960s, 835w, 791w, 760m, 741m, 728m, 697w, 675w, 650w, 506w. vw136s. Raman: 1576w, 1563w, sh, 1447s, 1469s, 1414s, 1335w, 1259w, 1159vw, 1093vw, 971vw, 654m, 531w, 539w, 336w, 253m, br, 137s, br, 92s.

[1,1'-Methylenebis(1,3-dimethyl-2(3H)-imidazolethione)]di-N-thiocyanatolead(II)

A similar procedure was used to prepare this compound. Hot ethanol was used to wash the dried, crude product which was obtained in *c*. 50% yield or less. The resultant tan powder was too insoluble for solution studies and did not yield crystallographic grade crystals. m.p. 254–256 °C. *Anal.* Calc. for $C_{11}H_{12}N_6PbS_4$: C, 23.44; H, 2.14; N, 14.91. Found: C, 23.43; H, 2.13; N, 14.88%. IR (Nujol mull): 2051s, 1563w, 1310s, 1261w, 1225s, 1204m, 1154s, 1090w, 1069w, 1045w, 960w, 930vw, 916vw, 820w, 790m, 763s, 716s, 690m, 669m, 648m, 528w, 506w, 477w, 461w. Raman: 2059s, 1570w, 1473w, 1437m, 1362m, 1263wm, 1205w, 1091vw, 1017vw, 763vw, 728vw, 651w, 509vw, 130m.

X-ray crystallographic data

Suitable crystals of $PbCl_2$mbit were mounted on a glass fiber using epoxy cement such that the longest crystal dimension was approximately parallel to the fiber axis. Unit cell parameters were determined on a Syntex $P2_1$ four circle diffractometer equipped with a graphite monochromator (Bragg 2θ angle = 12.2°) using Mo Kα ($\lambda = 0.71069$ Å) radiation at a takeoff angle of 6.75°. Fifteen reflections were machine centered and used in least-squares refinement of the lattice parameters. Omega scans of several low 2θ angle reflections gave peak widths at half-height of less than 0.24 Å indicating a satisfactory mosaic spread for the crystal examined. Axial photographs were used to determine the space group with zero and upper level intensity data being examined for systematic absences in the usual fashion.

Intensity data were collected using ω scans with X-ray source and monochromator settings identical to those used for determination of the unit cell parameters. A variable scan rate of 3.91 to 29.3° min^{-1} was used, and a scan width of 1.0° was sufficient to collect all the peak intensity. Stationary background counts were measured at the beginning and at the end of each scan with a total background-to-scan time ratio of 1.0. No significant fluctuations were observed in the intensities of three standard reflections measured every 100 reflections. Intensities were calculated from the total scan count and background counts by the usual relationship.

The intensities were assigned standard deviations in the usual manner, and intensity data are summarized in Table 1. Reflections were collected in a complete quadrant ($\pm h+k+l$) out to $2\theta = 50°$. Reflections were accepted as statistically above background on the basis that F was greater than $2.5\sigma(F)$. Lorentz and polarization corrections were made in the usual way. A psi-zero correction was made for absorption.

Solution and refinement of the structure

Computations were performed using the standard programs [3], and were carried out on the CDC Cyber 74 System. For structure factor calculations, the scattering factors were taken from the International Tables for X-ray Crystallography [4]. The agreement factors are defined in the conventional way. In all least-squares refinements, the quantity minimized has been previously defined [5]. The weighting schemes based on counting statistics are also as previously defined for the calculation of R_w and in least-squares refinement [5].

The structure was solved using a Patterson map. Hydrogen atoms were not added. Final calculated values for R and R_w as well as other crystallographic data are summarized in Table 1. Table 2 lists final positional parameters for the non-hydrogen atoms. Interatomic distances for the metal coordination sphere are seen in Fig. 3 while the angles are listed in Table 3. Table 3 also lists non-bonded contacts in the lead coordination sphere. Table 4 lists interatomic distances and angles for the ligand moiety. See also 'Supplementary material'.

TABLE 1. Data collection and processing parameters

Molecular formula	$C_9H_{12}Cl_2N_4PbS_2$
Molecular weight	518.45
Unit cell parameters	
a (Å)	8.699(3)
b (Å)	17.164(4)
c (Å)	20.469(6)
V (Å^3)	3056.2
Z	8
$F(000)$	1472
λ(Mo Kα) (Å)	0.71073
μ(Mo Kα) (mm^{-1})	11.58
Temperature (K)	294
Density (calc.) (g/cm^3)	2.254
Density (obs.) (g/cm^3)	2.23
Space group	*Pbca*
Crystal size (mm)	1.16×0.09×0.05
Unique data measured	2696
Observed data with $\lvert F_o\rvert > 2.5\sigma\lvert F_o\rvert$	1586
Conventional R	0.047
Weighted R	0.043
Goodness of fit	1.650
Residual electron density	−1.710/+1.390
Max. shift/error ratio final cycle	<0.006

TABLE 2. Atomic parameters x, y, z ($\times 10^4$) and isotropic temperature factors B_{iso} for atoms of $PbCl_2$mbit with e.s.d.s given in parentheses (hydrogen atoms omitted)

	x	y	z	B_{iso}
Pb	1679(1)	1159(1)	2170(1)	2.48(2)
S1	3628(4)	1896(2)	1108(2)	2.6(2)
S2	1081(4)	293(2)	1038(2)	2.8(2)
Cl1	4527(4)	142(2)	2202(2)	3.2(2)
Cl2	−681(5)	2177(3)	1895(2)	4.5(2)
N1	1054(14)	2655(6)	424(5)	2.8(5)
N2	2441(12)	3365(6)	1189(5)	2.3(5)
N3	162(11)	−1109(7)	1558(5)	2.2(5)
N4	−1731(13)	−403(6)	1219(5)	2.5(5)
C1	2520(15)	2645(7)	930(6)	2.1(6)
C2	836(16)	3377(9)	370(7)	3.0(7)
C4	3335(16)	3643(7)	1749(6)	2.5(5)
C5	−202(17)	−415(8)	1283(6)	2.6(6)
C6	−1197(16)	−1511(8)	1693(6)	2.5(6)
C7	−2343(16)	−1057(8)	1478(7)	2.9(6)
C8	1179(21)	1195(8)	0004(8)	4.9(9)
C9	−2552(18)	258(9)	925(8)	4.3(8)

TABLE 3. Interatomic angles (°) and non-bonding contacts (Å) in coordination sphere of lead with e.s.d.s given in parentheses. See Fig. 3 for atom designators

S1–Pb–S2	76.4(2)	S1···S2	3.546(6)
S1–Pb–Cl1	77.9(2)	S1···Cl1	3.749(6)
S1–Pb–Cl2	90.0(2)	S1···Cl2	4.054(7)
S1–Pb–Cl2″	77.3(2)	S1···Cl2″	4.013(7)
S2–Pb–Cl1	82.1(2)	S2···Cl1	3.834(6)
S2–Pb–Cl2	91.6(2)	S2···Cl2	3.984(7)
S2–Pb–Cl1′	85.9(2)	S2···Cl1′	3.859(7)
Cl1–Pb–Cl1′	100.1(2)	Cl1···Cl1′	4.520(3)
Cl1–Pb–Cl2″	74.8(2)	Cl1···Cl2″	3.958(6)
Cl2–Pb–Cl1′	89.5(2)	Cl2···Cl1′	3.958(6)
Cl2–Pb–Cl2″	106.7(2)	Cl2···Cl2″	5.005(5)
Cl1′–Pb–Cl2″	119.5(2)	Cl1′···Cl2″	5.224(7)
S1–Pb–Cl1′	162.3(2)		
Cl1–Pb–Cl2	168.2(2)		
S2–Pb–Cl2″	148.0(2)		

Results and discussion

The direct combination of equimolar quantities of PbX_2(X = Cl, SCN) and mbit in boiling water yielded high melting 1:1 complexes upon cooling. The crude products initially obtained were highly contaminated with unreacted mbit, hence the necessity of washing with organic solvents such as CH_2Cl_2 or hot ethanol. $PbCl_2$mbit was somewhat soluble in hot water, but insoluble in organic solvents of low polarity. $Pb(NCS)_2$mbit was too insoluble in any of the solvents tested and therefore could not be recrystallized or studied in solution state. The proton NMR of $PbCl_2$mbit in CD_3CN showed no significant difference from the ligand in the free state which may indicate complete or nearly complete dissociation in solution as was the

TABLE 4. Interatomic distances (Å) and angles (°) for ligand with e.s.d.s given in parentheses. See Fig. 4 for atom designators

S1–C1	1.678(13)	N2–C2–C3	106.0(12)	S2–C5–N3	126.1(11)
S2–C5	1.724(14)	N2–C4–N3	111.6(10)	S2–C5–N4	127.2(11)
N1–C1	1.362(17)	C1–N1–C3	110.3(10)	N3–C5–N4	106.6(11)
N1–C3	1.372(18)	C1–N1–C8	124.5(10)	N3–C6–C7	106.1(12)
N1–C8	1.450(17)	C3–N1–C8	125.1(12)	N4–C7–C6	108.6(12)
N2–C1	1.346(16)	C1–N2–C2	110.5(11)		
N2–C2	1.407(17)	C1–N2–C4	125.5(11)		
N2–C4	1.466(16)	C2–N2–C4	124.0(10)		
N3–C4	1.430(17)	C4–N3–C5	126.1(11)		
N3–C5	1.355(18)	C4–N3–C6	125.0(11)		
N3–C6	1.396(18)	C5–N3–C6	108.6(11)		
N4–C5	1.377(19)	C5–N4–C7	109.9(12)		
N4–C7	1.351(17)	C5–N4–C9	122.4(11)		
N4–C9	1.469(18)	C7–N4–C9	127.6(12)		
C2–C3	1.324(20)	S1–C1–N1	127.7(10)		
C6–C7	1.339(21)	S1–C1–N2	127.5(10)		
		N1–C1–N2	104.8(10)		
		N1–C3–C2	108.3(12)		

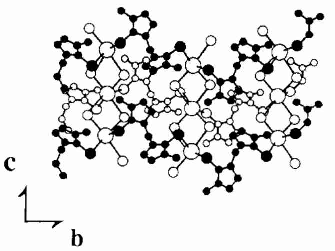

Fig. 2. Perspective of $PbCl_2$mbit viewed along the *b* and *c* axes. Darkened spheres depict ligand molecules projected out of the *b–c* plane along the *a* axis while open spheres represent ligand molecules behind the plane from this view.

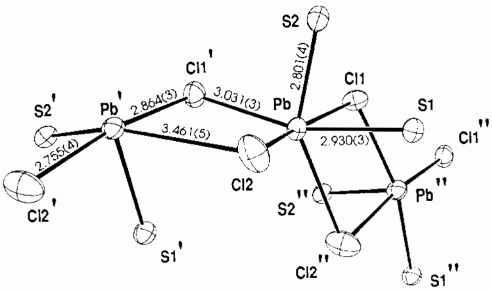

Fig. 3. ORTEP drawing of coordination sphere for metal. Thermal ellipsoids are drawn at the 50% probability level.

case for several thiourea-type complexes of other main group lower oxidation state halides [2, 6]. Low solubility of these complexes hampered attempts at other solution studies such as molecular weight or conductivity determinations.

The results from the single crystal X-ray study are shown in Figs. 2, 3 and 4. As seen in Fig. 2, $PbCl_2$mbit has a unique cross-linked polymeric structure composed of very distorted $PbCl_4S_2$ octahedra sharing common edges through long Pb-Cl bridges. The bridging pairs of Cl atoms are displaced *cis* to each other in the coordination sphere of lead thus creating twisted polymeric Pb–Cl strands running along the *c* axis. In the direction of the *b* axis, the strands are further linked by mbit ligands acting as bridges between neighboring twisted strands created by the lead chloride bonds. This is the first instance where mbit is shown to act as a bridging ligand. As mentioned above, the only other structural study to date involving mbit was reported for $SbCl_3$mbit in which the ligand bonded in a bidentate fashion.

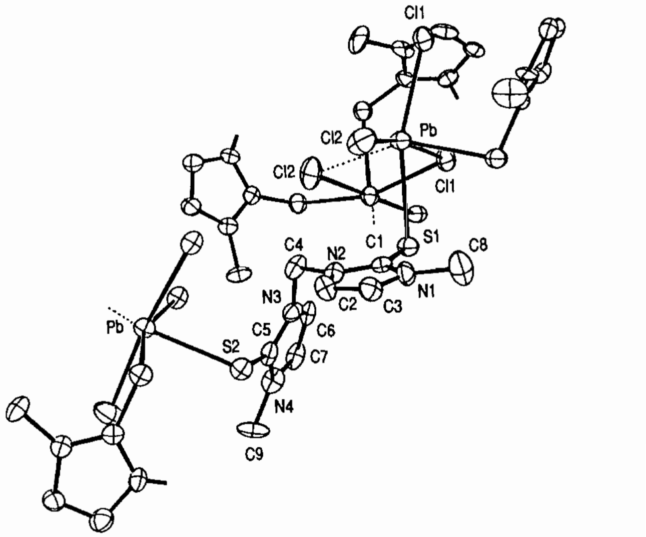

Fig. 4. ORTEP drawing showing bridging ligand moiety and atom designators. Thermal ellipsoids are drawn at the 50% probability level.

The type of polymerization described above is reminiscent of that observed for $Pb(dtp)_2$ (dtp=*O,O'*-diisopropylphosphorodithiolate) [7] where long bridging Pb-S bonds link the individual PbS_6 units together. There is no cross-linking, however, in $Pb(dtp)_2$. Figure 3 shows the very highly distorted octahedral site symmetry around lead. Almost linear covalent $PbCl_2$ units (168.18°) link to each other by very long chlorine bridges (3.031 and 3.461 Å) bonding *cis* to each other and displaced in such a fashion from unit to unit so as to create the twisted polymeric strands described above. Sulfur atoms from different ligands bond *cis* to each other in the coordination sphere of lead thus giving the cross-link effect running along the orthogonal *b* axis. From the bond distances and angles reported in Fig. 2 and Table 3, respectively, it can be seen that the local site symmetry around the lead atom is best described as distorted octahedral. Bond angles range from 74.80° (C11–Pb–C12″) to 119.49° (C11′–Pb–C12″). Two other exceptionally large positive deviations from 90° are seen with C12–Pb–C12″ and C11′–Pb–C11 at 106.70° and 100.02°, respectively. Correspondingly large

Cl···Cl non-bonded distances are also observed with Cl1′···Cl2″ at 5.224 Å, Cl2···Cl2″ at 5.005 Å and Cl1···Cl1′ at 4.520 Å. There are also three other large negative deviations from 90° observed with S1–Pb–S2, S1–Pb–Cl1 and S1–Pb–Cl2″ at 76.41°, S1–Pb–Cl2 at 77.29°, and S1–Pb–Cl2 at 77.29°, and S1–Pb–Cl1 at 77.89°. This systematic distortion pattern of one triangular face of the octahedron splayed open with another face tightened down is similar to the coordination geometry around Bi in Bi(dtp)$_3$ [8]. The observed distortion pattern may be the result of the non-bonded lone pair of electrons in the valence shell of lead, but this is purely speculative given the sheer bulk and somewhat rigid nature of the mbit ligand along with the penchant of Pb(II) to attain higher coordination numbers through polymerization thus making this distortion simply the result of the most efficient crystal packing mode possible. Nevertheless, the unique cross-linked polymeric structure accounts for the high melting point and low solubility properties of this particular complex.

Figure 4 shows a more detailed picture of the ligand configuration and its position relative to the lead centers. The ligand interatomic distances and angles compared favorably to those noted in the structure of SbCl$_3$mbit with of course the obvious conformational differences focused primarily around the connecting methylene carbon (C4). Several conventional least-squares plane calculations indicate a high degree of planarity for the mbit rings.

The only structural evidence available for Pb(SCN)$_2$mbit is the FT-IR spectrum which shows the characteristic strong ν(CN) peak at 2051 cm^{-1} and ν(CS) peak at 820 cm^{-1}, well within the range associated with N-bonded thiocyanate moieties in lead(II) complexes [9]. The NCS deformation mode appears to be at 461 cm^{-1} which is slightly below the range observed by Baranyi *et al.* [9], but closer to 480 cm^{-1}, the value observed for several N-bonded complexes of other metals [10]. It appears, therefore, that the thiocyanate group is not bridged, but from the very high melting point and low solubility, the structure would appear to be polymeric, perhaps linked through the mbit ligands only.

Supplementary material

Additional tables of structure factors and thermal parameters are available from author D.J.W.

Acknowledgements

D.J.W. thanks the Kennesaw College Faculty Development Fund and the Wilcom Foundation of Marietta, GA (USA) for partial support of this research. We also thank Dr Martha C. Williams of the Wilcom Foundation for her help in computational programming, and we are grateful to Professor Nai-Teng Yu of Georgia Tech for the use of the FT-Raman spectrophotometer.

References

1 D. J. Williams, D. VanDerveer, R. L. Jones and D. S. Menaldino, *Inorg. Chim. Acta, 165* (1989) 173.

2 D. J. Williams, R. L. Jones and P. H. Poor, *Inorg. Chim. Acta, 144* (1988) 237.

3 E. J. Gabe, F. L. Lee and Y. Le Page in G. M. Sheldrick, C. Kruger and R. Goddard (eds.), *Crystallographic Computing 3: Data Collection, Structure Determination, Proteins, and Databases,* Clarendon Press, Oxford, 1985, pp. 167–174.

4 *International Tables for X-ray Crystallography*, Vol. IV, Kynoch, Birmingham, UK, 1974.

5 D. J. Williams, G. Ramirez and D. VanDerveer, *J. Crystallogr. Spectrosc. Res., 16* (1986) 309.

6 D. J. Williams and K. J. Wynne, *Inorg. Chem., 17* (1978) 1108.

7 S. L. Lawton and G. T. Kokotailo, *Inorg. Chem., 11* (1972) 363.

8 S. L. Lawton, C. J. Fuhrmeister, R. G. Haas, C. A. Jarman, Jr. and F. G. Lohmeyer, *Inorg. Chem., 13* (1974) 135.

9 A. D. Baranyi, R. Makhija and M. Onyszchuk, *Can. J. Chem., 54* (1976) 1189.

10 K. Nakamoto, *Infrared and Raman Spectra of Inorganic and Coordination Compounds,* Wiley–Interscience, New York, 4th edn., 1986, p. 283.